Research Square

Preprints are preliminary reports that have not undergone peer review.
They should not be considered conclusive, used to inform clinical practice,
or referenced by the media as validated information.

A head-to-head comparison of MM/PBSA and MM/GBSA in predicting binding affinities for the CB_1 cannabinoid ligands

Mei Qian Yau

meiqian.yau@taylors.edu.my

Taylor's University

Clarence W.Y. Liew

Taylor's University

Jing Hen Toh

Taylor's University

Jason S.E. Loo

Taylor's University

Research Article

Keywords: Binding affinity, CB1 cannabinoid receptor, MM/PBSA, MM/GBSA, molecular dynamics

Posted Date: June 25th, 2024

DOI: https://doi.org/10.21203/rs.3.rs-4539129/v1

License: This work is licensed under a Creative Commons Attribution 4.0 International License.
Read Full License

Additional Declarations: No competing interests reported.

Version of Record: A version of this preprint was published at Journal of Molecular Modeling on October 31st, 2024. See the published version at https://doi.org/10.1007/s00894-024-06189-4.

Abstract

The substantial increase in the number of active and inactive-state CB_1 receptor experimental structures has provided opportunities for CB_1 drug discovery using various structure-based drug design methods, including the popular end-point methods for predicting binding free energies – Molecular Mechanics/Poisson-Boltzmann Surface Area (MM/PBSA) and Molecular Mechanics/Generalized Born Surface Area (MM/GBSA). In this study, we have therefore evaluated the performance of MM/PBSA and MM/GBSA in calculating binding free energies for CB_1 receptor. Additionally, with both MM/PBSA and MM/GBSA being known for their highly individualized performance, we have evaluated the effects of various simulation parameters including the use of energy minimized structures, choice of solute dielectric constant, inclusion of entropy, and the effects of the five GB models. Generally, MM/GBSA provided higher correlations than MM/PBSA ($r_{MM/GBSA}$ = 0.433 – 0.652 vs. $r_{MM/PBSA}$ = 0.100 – 0.486) regardless of the simulation parameters, while also offering faster calculations. Improved correlations were observed with the use of molecular dynamics ensembles compared with energy-minimized structures and larger solute dielectric constants. Incorporation of entropic terms led to unfavorable results for both MM/PBSA and MM/GBSA for a majority of the dataset, while the evaluation of the various GB models exerted a varying effect on both the datasets. The findings obtained in this study demonstrate the utility of MM/PBSA and MM/GBSA in predicting binding free energies for the CB_1 receptor, hence providing a useful benchmark for their applicability in the endocannabinoid system as well as other G protein-coupled receptors.

INTRODUCTION

Cannabis sativa, widely known as marijuana, is a medicinal plant containing psychotropic compounds that has been used for both recreational and medical purposes for centuries. While the utility of marijuana for medicinal purposes has garnered heated debates, following the first approval of a cannabinoid compound, dronabinol, for medicinal use in 1991 [1], a number of countries and states have legalized its therapeutic use [2]. The pharmaceutical properties of marijuana are derived from its active ingredient, Δ^9-tetrahydrocannabinol (Δ^9-THC) [3]. The discovery of Δ^9-THC subsequently led to the identification of endogenous ligands that bind to the CB_1 and CB_2 cannabinoid receptors [4, 5], thereby forming the endocannabinoid system [6–9]. Both the CB_1 and CB_2 receptors are G protein-coupled receptors (GPCRs), which constitutes the largest superfamily of membrane proteins in the human genome [10]. The CB_1 receptor can be predominantly found in the central nervous system while the CB_2 receptor is mostly expressed in the immune system [11]. The receptors therefore play major roles in the human body where they are known to mediate a wide range of biological processes including pain, inflammation, metabolic disorders, cancer, cardiovascular conditions, and neurodegenerative disorders [12–14].

Over the years, numerous efforts have been made in exploiting the therapeutic potential of the cannabinoid receptors, notably the CB_1 receptor. This has resulted in the synthesis of phytocannabinoids

and synthetic cannabinoids that possess varying affinities for numerous clinical conditions [14]. However, only a handful of these drugs are clinically approved due to their side effects. For example, compounds targeting the CB_1 receptor have demonstrated therapeutic utilities in treating chemotherapy-induced nausea and vomiting, as well as spasticity in multiple sclerosis [15, 16]. However, their expression in the central nervous system led to psychiatric side effects, thus causing several inverse agonists targeting the CB_1 receptor to be withdrawn from the market, such as rimonabant and taranabant [17, 18]. Hence, there is a need for the discovery of novel synthetic CB_1 ligands with better therapeutic profiles.

For many years, the drug discovery industry experienced severe limitations in obtaining high quality experimental structures for the CB_1 receptor due to the inherent membrane-bound characteristic of GPCRs [19]. Nevertheless, advancements in X-ray crystallography as well as the introduction of cryo-electron microscopy led to GPCR experimental structures being solved in an increasingly fast pace [20, 21]. To date, 1160 GPCR experimental structures have been made available in the Protein Data Bank (PDB) and this includes 19 CB_1 cannabinoid receptors [22] in both their active and inactive-states, which are coupled with agonists, antagonists, inverse agonists, allosteric modulators, and G_i subunit [23–30]. The rapid expansion of the number of experimental structures has therefore propelled structure-based drug design (SBDD) investigations on the structures and functions of the cannabinoid receptors, including binding affinity prediction and virtual screening studies [31–36].

In SBDD, binding free energies are often used to determine the binding strength of a receptor-ligand complex [37]. A well-known end-point free energy method for predicting binding free energies, Molecular Mechanics/Poisson-Boltzmann Surface Area (MM/PBSA) and its close counterpart Molecular Mechanics/Generalized Born Surface Area (MM/GBSA) have continuously been utilized to efficiently predict binding free energies for various complexes, as they are relatively accurate and computationally inexpensive in comparison to the fast but inaccurate scoring functions employed in molecular docking programs and highly accurate but computationally costly alchemical pathway free energy methods [38]. Using the single-trajectory approach for MM/PB(GB)SA calculation, molecular dynamics (MD) simulations of the protein-ligand complex are typically first performed in an explicit water environment, followed by the removal of the water molecules during binding free energy prediction of the complex which can be calculated as shown in Eq. 1.

$$\Delta G_{bind} = G_{complex} - \left(G_{protein} + G_{ligand}\right)$$

1

For each component in Eq. 1, the free energy can be calculated as below:

$$G = E_{MM} + G_{PB/GB} + G_{SA} - TS_{solute}$$

2

where E_{MM} represents the gas-phase molecular mechanics (MM) term that can be derived from the sum of electrostatic (E_{ele}), van der Waals (E_{vdW}) and internal (E_{int}) energies, $G_{PB/GB}$ is the continuum solvent Poisson-Boltzmann (PB) or Generalized Born (GB) model for polar solvation, G_{SA} is the solvent-accessible surface area (SA) dependent nonpolar solvation term, and TS_{solute} is the solute entropy term. The PB model stands as a popular choice in molecular simulations owing to its accuracy in estimating polar solvation energies. However, in recent years the GB model has gained traction as a computationally efficient alternative, particularly for large-scale simulations as it provides a simplified approximation to calculating solvation energies. The PB model solves the Poisson-Boltzmann equation by taking into account the electrostatic interactions between the solute and solvent molecules while the GB model simplifies this approach by approximating solvation energies based on the Generalized Born theory, which considers the effective Born radii of atoms and the dielectric properties of the environment [39]. Therefore, careful consideration must be given to their respective applicability as they differ in their complexity. Factors such as accuracy, computational resources, and system size play a pivotal role in determining the suitability of these methods for calculating solvation energies.

The utility of both MM/PBSA and MM/GBSA in structure-based drug design applications such as binding free energy prediction, rescoring docked poses, virtual screening, and consensus scoring, has been widely demonstrated [36, 40–45]. A prior study has calculated MM/PBSA and MM/GBSA binding free energies for a set of CB_1 agonists and antagonists [34]. However, as the study utilized separate modules to predict MM/PSBA and MM/GBSA binding free energies (*g_mmpbsa* for MM/PBSA and Prime-MM/GBSA for MM/GBSA), there remains room to systematically assess and compare the performance of MM/PBSA and MM/GBSA as the use of different modules essentially requires different implementations of the algorithms and parameterization schemes including force fields and solvation effects. In addition, the performance of MM/PBSA and MM/GBSA has been known to be highly system- and parameter-dependent. For example, a binding affinity prediction study has reported varied correlation coefficients ranging from − 0.42 to 0.92 for six different protein systems [45]. Therefore, in this study, we have provided a direct comparison of the performance of MM/PBSA and MM/GBSA in predicting binding free energies for CB_1 agonists and antagonists. We have additionally systemically assessed the effects of various simulation parameters on the performance of MM/PBSA and MM/GBSA to accurately predict binding free energies.

METHODS

Dataset selection and preparation

The CB_1 dataset from Loo *et al.* was utilized to provide a comparative assessment of the performance of MM/PBSA and MM/GBSA [34]. Briefly, the dataset consists of 46 ligands, 23 of which are agonists and 23 are antagonists. The ligands, obtained from the ChEMBL database [46], were of a congeneric series and the experimental binding affinities of the ligands spanned from 0.1 nM to > 1000 nM. The ligands were prepared using LigPrep [47]. The crystal structures of the active-state CB_1 receptor-CB_1 agonist

AM11542 (PDB ID: 5XRA) and inactive-state CB_1 receptor-CB_1 antagonist AM6538 (PDB ID: 5TGZ) were obtained from the Protein Data Bank (PDB) [23, 26, 48]. The structures were prepared using Protein Preparation Wizard in Maestro [49], and Epik was used to assign suitable protonation and tautomeric states [50], followed by optimization of hydrogen bonds and restrained energy minimization prior to docking. The ligands were docked to their respective crystal structure using the Induced Fit Docking protocol with Glide XP scoring function [51, 52]. Binding poses that were best aligned to the respective crystal structure ligand were selected for subsequent MD simulations and MM/PBSA calculations. These structures were utilized without subsequent modifications.

Molecular dynamics simulations

The equilibrated structures from Loo *et al.* were subjected to MD simulations using GROMACS 2018 [53]. AMBER ff99SB*-ILDN was used for the proteins [54], while General Amber Force Field (GAFF) was used for the ligands (Wang et al., 2004), and Slipids parameters for lipids [56]. Ligand topologies were generated using *acpype* with the AM1-BCC method to calculate partial charges [57, 58]. Lennard-Jones (LJ) and short-range electrostatic interactions were truncated at 10 Å, while the Particle-Mesh-Ewald (PME) algorithm was used to calculate the long-range electrostatic interactions [59]. Hydrogen bonds were constrained using LINCS [60, 61]. The POPC bilayer was generated using CHARMM-GUI and aligned using the Orientations of Proteins in Membrane database [62, 63]. The complexes were then solvated using TIP3P water molecules and neutralized by 0.15 M NaCl [64], followed by energy minimization. Next, the systems were equilibrated for 100 ps at 300 K in the NVT ensemble using the Berendsen thermostat, followed by 10 ns at 300 K and 1 atm in the NPT ensemble using the Berendsen barostat and thermostat with the heavy atoms of the complexes being restrained with a force constant of 1000 kJ/mol nm^2 [65]. These equilibrated structures were subsequently utilized for 30 ns production simulations at 300 K and 1 atm with the velocity rescaling thermostat and the Parinello-Rahman barostat [66, 67].

MM/PBSA & MM/GBSA calculations

MM/PBSA and MM/GBSA binding free energy calculations were performed using gmx_MMPBSA [68] for both the initial energy minimized and molecular dynamic simulations structures, where the first 2 ns of the simulations were removed and frames were obtained every 100 ps, resulting in a total of 280 frames for each complex (Fig. 1). Correlations between the experimental and MM/PB(GB)SA predicted binding free energies were measured using Pearson correlation coefficients, *r*. The effect of entropy on MM/PB(GB)SA binding free energies were evaluated using the interaction entropy module implemented in gmx_MMPBSA (68). The solute dielectric constant, ε, was varied between 1, 2, and 4 to study the effect of different solute dielectric constants on the performance of MM/PB(GB)SA. For MM/GBSA calculations, five GB models (igb = 1, 2, 5, 7, 8) that are available within gmx_MMPBSA were systematically evaluated to explore the effect of the choice of GB models in the performance of MM/GBSA [39, 69–71]. The GB models 1, 2, 5, 7, and 8 correspond to GB^{HCT}, GB^{OBC1}, GB^{OBC2}, GB^{Neck}, and GB^{Neck2} respectively. The differences between these models lie mainly in their parameterization

including the treatment of solvent molecules and size of atomic radii, as well as their applications in complexes of various sizes, leading to various observed effects in other protein systems [45].

RESULTS AND DISCUSSION

Comparison of the performance of MM/PBSA and MM/GBSA in binding affinity prediction for CB_1 receptor agonists and antagonists

MM/PBSA obtained a wide range of correlations between predicted and experimental binding free energies, with *r* ranges of 0.100–0.486 for the agonist dataset and 0.363–0.481 for the antagonist dataset when evaluated using various parameters. Similarly, when evaluated across the different parameters, MM/GBSA obtained an extensive range of correlations with *r* of 0.433–0.652 for the agonist dataset and 0.450–0.600 for the antagonist dataset. Figure 2 shows the correlations obtained using MM/PBSA and MM/GBSA when evaluated across different parameters. Comparatively, Glide obtained a modest correlation of 0.384 for the agonist dataset and a slightly more notable correlation of 0.610 for the antagonist dataset. When considering the default MM/PBSA and MM/GBSA parameters (ε = 1, GB model = 5), MM/GBSA obtained an improvement from Glide with increase in *r* of 0.175 for the agonist dataset, while a slight decline of 0.046 was observed for the antagonist dataset. On the other hand, MM/PBSA showed declines of 0.061 and 0.129 for the agonist and antagonist datasets respectively. With MM/PSBA demonstrating a majority decline in correlations for both datasets and MM/GBSA showing only improvements in the agonist dataset in comparison to Glide (Fig. 3), this emphasizes the superior performance of Glide rather than the subpar performance of MM/PBSA and MM/GBSA, as reflected in prior studies [40, 41]. While the accuracy of the initial docking pose may play a role in binding free energy estimations using MM/PB(GB)SA [36], both the datasets utilized in this study have demonstrated excellent agreement between the docked ligands and the crystallographic ligands [34], hence providing an equitable basis for binding free energy predictions. Another factor to consider is the choice of force field employed in this study; Glide employs the OPLS force field whereas AMBER was utilized in MM/PBSA and MM/GBSA. Prior investigations assessing free energy methods have demonstrated enhanced outcomes associated with the use of OPLS [72, 73], thus reinforcing the higher Glide correlations in this study. Nevertheless, the results clearly demonstrated the superiority of the performance of MM/GBSA in comparison to MM/PBSA. This ability of MM/GBSA to better predict relative binding free energies is consistent with previous studies [74, 75]. However, with both MM/PBSA and MM/GBSA obtaining a wide range of correlations, this further emphasises the highly system- and parameter-dependent performance of the MM/PBSA and MM/GBSA methods in predicting binding free energies [41, 76, 77]. We have therefore evaluated the effects of various parameters on the performance of MM/PBSA and MM/GBSA.

Effects of various parameters on the performance of MM/PBSA and MM/GBSA

Effect of using energy minimized versus molecular dynamics structures

The performance of both MM/PBSA and MM/GBSA improved with the use of MD structures. A more prominent improvement in correlation was obtained using MM/PBSA in comparison to MM/GBSA with differences in correlation of up to 0.223 for MM/PBSA and 0.112 for MM/GBSA. These results are consistent with prior studies indicating that the ability of MD simulations to explore the configurational space and provide an ensemble of protein-ligand binding conformations may be beneficial towards improving approximations, in comparison to EM where only one static state of the complex is utilized for the calculations [78, 79]. This is further made more prominent when utilising docked poses in comparison to experimental structures as a starting point for MM/PBSA and MM/GBSA calculations, such as those used in this study, as docked poses typically require further refinement and equilibration using MD simulations in order to obtain better MM/PBSA and MM/GBSA correlations [76]. However, the modest improvements in correlations ($r < 0.3$) achieved through MD simulations must be weighed against the substantial increase in computational cost required for their implementation. Previous investigations have demonstrated comparable correlations between EM and MD structures therefore suggesting the viability of using EM structures in large-scale virtual screening studies, thereby mitigating the computational cost associated with such endeavors [36, 80].

Effect of using different solute dielectric constant values

Increasing the solute dielectric constant (ε) provided slight improvements for the majority of the datasets. The results are consistent with that obtained from the previous study whereby it has been reported that the lower correlations obtained at ε = 1 were attributed to the overestimation of the polar solvation energy [34]. Generally, the use of larger solute dielectric constants is recommended when the binding site of the receptor or ligand used is more polar in nature to avoid the overestimation of electrostatic interactions [81, 82]. However, both the CB_1 receptors' binding pockets and its ligands are hydrophobic in nature. It was therefore surprising in this study whereby improved correlations were observed with increasing ε. As reported in the previous study, the reason behind this unusual finding may be due to the presence of polar substituents in the ligand datasets utilised therefore leading to an augmentation in the solvation energies approximation [34]. For example, the average aggregate of the polar solvation energy reduced by 20 kcal/mol and 18 kcal/mol for MM/PBSA and MM/GBSA respectively when the ε increases from 1 to 4 for the agonist dataset, while an average reduction of 21 kcal/mol and 16 kcal/mol were observed for MM/PBSA and MM/GBSA respectively with increasing ε for the antagonist dataset. This therefore implies that irrespective of the receptor characteristics, the predominant cause of the lower correlations at ε = 1 is the overvaluation of polar solvation energies. Similarly, other systematic assessments have also reported the enhanced performance of MM/PBSA using higher solute dielectric constants [34, 74, 76]. Therefore, based on our findings, we suggest that choosing a higher solute dielectric constant instead of the common default of ε = 1 may be a more rational approach in both MM/PBSA and MM/GBSA calculations, especially for the CB_1 system.

Effect of incorporating interaction entropy

The inclusion of interaction entropy in MM/PBSA and MM/GBSA calculations generally led to declines in correlations for both the agonist and antagonist datasets. Nonetheless, slight improvements were seen in the agonist dataset when using ε = 1 for MM/GBSA calculations with the inclusion of interaction entropy. A similar effect has been demonstrated in another study for the HIV-1 system, in which higher correlations were observed when ε is within the range of 1.4–1.6 for MM/PBSA and 1.8–2.0 for MM/GBSA [83], while ε = 1 provided optimum MM/GBSA binding free energies for the factor Xa system [84], therefore indicating the importance of considering the effects of solute dielectric constants during entropy calculations for different protein systems in order to obtain optimum binding free energies for individual targets [85, 86]. However, with only one dataset experiencing such improvements, one such explanation for the declines in correlations could possibly be due to the overestimation of entropic penalty for charged ligands as well as the flexibility of the ligands dataset as interaction entropy was built on the assumption that both protein and ligand maintained the same configurations before and after binding [87, 88]. The results from this study provided no clear trends on the benefits of incorporating interaction entropy during MM/PBSA and MM/GBSA calculations with improvements of only ($r \leq 0.1$). This is coherent with other studies which demonstrated relatively poor correlations when including entropy effects during MM/PBSA and MM/GBSA calculations, irrespective of employing the more computationally intensive normal-mode analysis of entropy or the more expedient interaction entropy method [83, 88]. This therefore necessitates careful validation of the system of interest when optimizing the use of interaction entropy for MM/PBSA and MM/GBSA binding free energy calculations.

Effect of the different GB models

The evaluation of the various GB models implemented in gmx_MMPBSA revealed mixed results. For the agonist dataset, the GB^{Neck} model provided the highest correlations across all dielectric constants, while the GB^{HCT} and GB^{OBC1} models provided equally poorer correlations. On the contrary, the GB^{HCT} model demonstrated the best performance for the antagonist dataset, while the GB^{Neck2} model performed poorly. With previous studies reporting newer models such as GB^{Neck} and GB^{Neck2} providing better performances over the traditional GB models [71, 89, 90], this was only applicable to the agonist dataset in this study, while the results from the antagonist dataset have demonstrated otherwise. The poor performance of the newer GB models in the antagonist dataset may be attributed to the lack of optimization of the models to protein-ligand systems, such as that applied in this study, as previous optimization efforts were aimed at protein-peptide systems [71, 91]. Furthermore, the choice of force field has been demonstrated to significantly impact the performance of different GB models [71, 92], underscoring the importance of specific parameter adjustments to ensure compatibility with the chosen GB model. However, with the varied performances of the GB models observed across the agonist and antagonist datasets, this further reinforces the importance of careful validation of the MM/GBSA parameters for individual protein systems. These varied results obtained were in line with a study which assessed the performance of three GB models (GB^{HCT}, GB^{OBC1}, and GB^{OBC2}) [45]. While the study

demonstrated that the GB^{OBC1} performed the best overall, GB^{OBC2} provided better correlations for the cytochrome C peroxidase system, indicating the highly individualized performance of the different GB models for various protein systems.

CONCLUSION

In this study, we have provided an assessment of the performance of MM/PBSA and MM/GBSA in predicting binding free energies for the CB_1 receptor. While we found that both MM/PBSA and MM/GBSA performed relatively poorly in comparison to docking, MM/GBSA outperformed MM/PBSA for both the agonist and antagonist datasets. The use of MD structures and larger solute dielectric constants provided improved correlations for both MM/PBSA and MM/GBSA. On the other hand, inclusion of interaction entropy led to significant declines, with the exception of MM/GBSA for the agonist dataset at $\varepsilon = 1$. The assessment of the various GB models provided varied effects with the GB^{Neck} and GB^{HCT} models providing the most positive effects for the agonist and antagonist datasets respectively. The varied results obtained here further highlight the system- and parameter-dependent characteristics of both MM/PBSA and MM/GBSA therefore necessitating the careful validation of these methods for the system of interest prior to utilization for binding free energy calculation of large virtual screening datasets. The outcomes from this study provide a standard reference on the applicability of MM/PBSA and MM/GBSA to predict binding free energies for the CB_1 receptor as well as other GPCR-associated targets.

Declarations

Competing interests

The authors have no relevant financial or non-financial interests to disclose.

Funding

The authors declare that no funds, grants, or other support were received during the preparation of this manuscript.

Author Contribution

All authors contributed to the study conception and design. Material preparation, data collection and analysis were performed by M.Q.Y, C.W.Y.L, and J.H.T. The first draft of the manuscript was written by M.Q.Y. J.S.E.L commented on previous versions of the manuscript. All authors approved the final manuscript.

Data availability

The simulation data, processed data, and code utilized in this study is available from the authors upon reasonable request.

References

1. Plasse TF. Clinical use of dronabinol. Journal of Clinical Oncology. 1991;9(11):2079–80. https://doi.org/10.1200/JCO.1991.9.11.2079
2. Pacula RL, Smart R. Medical marijuana and marijuana legalization. Annu Rev Clin Psychol. 2017;13:397–419. https://doi.org/10.1146/annurev-clinpsy-032816-045128
3. Mechoulam R, Gaoni Y. A total synthesis of dl-Δ1-Tetrahydrocannabinol, the active constituent of hashish. J Am Chem Soc. 1965;87(14):3273–5. https://doi.org/10.1021/ja01092a065
4. Munro S, Thomas KL, Abu-Shaar M. Molecular characterization of a peripheral receptor for cannabinoids. Nature. 1993;365:61–5. https://doi.org/10.1038/365061a0
5. Matsuda LA, Lolait SJ, Brownstein MJ, Young AC, Bonner TI. Structure of a cannabinoid receptor and functional expression of the cloned cDNA. Nature. 1990;346:561–4. https://doi.org/10.1038/346561a0
6. Marzo V di, Fontana A. Anandamide, an endogenous cannabinomimetic eicosanoid: “Killing two birds with one stone.” Prostaglandins Leukot Essent Fatty Acids. 1995;53:1–11. https://doi.org/10.1016/0952-3278(95)90077-2
7. Mechoulam R, Ben-Shabat S, Hanus L, Ligumsky M, Kaminski NE, Schatz AR, et al. Identification of an endogenous 2-monoglyceride, present in canine gut, that binds to cannabinoid receptors. Biochem Pharmacol. 1995;50(1):83–90. https://doi.org/10.1016/0006-2952(95)00109-D
8. Sugiura T, Kondo S, Sukagawa A, Nakane S, Shinoda A, Itoh K, et al. 2-arachidonolglycerol: A possible endogenous cannabinoid receptor ligand in brain. Biochem Biophys Res Commun. 1995;215(1):89–97. https://doi.org/10.1006/bbrc.1995.2437
9. Devane WA, Hanus L, Breuer A, Pertwee RG, Stevenson LA, Griffin G, et al. Isolation and structure of a brain constituent that binds to the cannabinoid receptor. Science (1979). 1992;258(5090):1946–9. https://doi.org/10.1126/science.1470919
10. Fredriksson R, Lagerström MC, Lundin LG, Schiöth HB. The G-protein-coupled receptors in the human genome form five main families. Phylogenetic analysis, paralogon groups, and fingerprints. Mol Pharmacol. 2003;63(6):1256–72. https://doi.org/10.1124/mol.63.6.1256
11. Howlett AC, Breivogel CS, Childers SR, Deadwyler SA, Hampson RE, Porrino LJ. Cannabinoid physiology and pharmacology: 30 Years of progress. Neuropharmacology. 2004;47(SUPPL. 1):345–58. https://doi.org/10.1016/j.neuropharm.2004.07.030
12. Wu J. Cannabis, cannabinoid receptors, and endocannabinoid system: yesterday, today, and tomorrow. Vol. 40, Acta Pharmacologica Sinica. Nature Publishing Group; 2019. p. 297–9.

https://doi.org/10.1038/s41401-019-0210-3

13. Mackie K. Cannabinoid receptors: Where they are and what they do. Journal of Neuroendocrinology. 2008. p. 10–4. https://doi.org/10.1111/j.1365-2826.2008.01671.x
14. Cristino L, Bisogno T, di Marzo V. Cannabinoids and the expanded endocannabinoid system in neurological disorders. Nat Rev Neurol. 2020;16(1):9–29. https://doi.org/10.1038/s41582-019-0284-z
15. Rock EM, Parker LA. Cannabinoids as potential treatment for chemotherapy-induced nausea and vomiting. Frontiers in Pharmacology. 2016;7:221. https://doi.org/10.3389/fphar.2016.00221
16. Giacoppo S, Bramanti P, Mazzon E. Sativex in the management of multiple sclerosis-related spasticity: An overview of the last decade of clinical evaluation. Mult Scler Relat Disord. 2017;17:22–31. https://doi.org/10.1016/j.msard.2017.06.015
17. Koch L. Taranabant no longer developed as an antiobesity agent. Nat Rev Endocrinol. 2010;6:300. https://doi.org/10.1038/nrendo.2010.56
18. Johansson K, Neovius K, Desantis SM, Rössner S, Neovius M. Discontinuation due to adverse events in randomized trials of orlistat, sibutramine and rimonabant: A meta-analysis. Obesity Reviews. 2009; 10:564–75. https://doi.org/10.1111/j.1467-789X.2009.00581.x
19. Ghosh E, Kumari P, Jaiman D, Shukla AK. Methodological advances: the unsung heroes of the GPCR structural revolution. Nat Rev Mol Cell Biol. 2015;16(2):69–81. https://doi.org/10.1038/nrm3933
20. Merk A, Bartesaghi A, Banerjee S, Falconieri V, Rao P, Davis MI, et al. Breaking cryo-EM resolution barriers to facilitate drug discovery. Cell. 2016;165(7):1698–707. http://dx.doi.org/10.1016/j.cell.2016.05.040
21. Shonberg J, Kling RC, Gmeiner P, Löber S. GPCR crystal structures: Medicinal chemistry in the pocket. Bioorg Med Chem. 2015;23(14):3880–906. http://dx.doi.org/10.1016/j.bmc.2014.12.034
22. Kooistra AJ, Mordalski S, Pandy-Szekeres G, Esguerra M, Mamyrbekov A, Munk C, et al. GPCRdb in 2021: integrating GPCR sequence, structure and function. Nucleic Acids Res. 2020;1–9. https://doi.org/10.1093/nar/gkaa1080
23. Hua T, Vemuri K, Nikas SP, Laprairie RB, Wu Y, Qu L, et al. Crystal structures of agonist-bound human cannabinoid receptor CB1. Nature. 2017;547(7664):468–71. https://doi.org/10.1038/nature23272
24. Wang X, Liu D, Shen L, Li F, Li Y, Yang L, et al. A genetically encoded F-19 NMR probe reveals the allosteric modulation mechanism of cannabinoid receptor 1. J Am Chem Soc. 2021;143(40):16320–5. https://doi.org/10.1021/jacs.1c06847
25. Hua T, Vemuri K, Pu M, Qu L, Han GW, Wu Y, et al. Crystal structure of the human cannabinoid receptor CB1. Cell. 2016;167(3):750-762.e14. https://doi.org/10.1016/j.cell.2016.10.004
26. Shao Z, Yin J, Chapman K, Grzemska M, Clark L, Wang J, et al. High-resolution crystal structure of the human CB1 cannabinoid receptor. Nature. 2016;540(7634):602–6. https://doi.org/10.1038/nature20613

27. Shao Z, Yan W, Chapman K, Ramesh K, Ferrell AJ, Yin J, et al. Structure of an allosteric modulator bound to the CB1 cannabinoid receptor. Nat Chem Biol. 2019;15(12):1199–205. https://doi.org/10.1038/s41589-019-0387-2
28. Hua T, Li X, Wu L, Iliopoulos-Tsoutsouvas C, Wang Y, Wu M, et al. Activation and signaling mechanism revealed by cannabinoid receptor-Gi complex structures. Cell. 2020;180(4):655-665.e18. https://doi.org/10.1016/j.cell.2020.01.008
29. Krishna Kumar K, Robertson MJ, Thadhani E, Wang H, Suomivuori CM, Powers AS, et al. Structural basis for activation of CB1 by an endocannabinoid analog. Nat Commun. 2023;14(1). https://doi.org/10.1038/s41467-023-37864-4
30. Krishna Kumar K, Shalev-Benami M, Robertson MJ, Hu H, Banister SD, Hollingsworth SA, et al. Structure of a signaling cannabinoid receptor 1-G protein complex. Cell. 2019;176(3):448-458.e12. https://doi.org/10.1016/j.cell.2018.11.040
31. Aviz-Amador A, Contreras-Puentes N, Mercado-Camargo J. Virtual screening using docking and molecular dynamics of cannabinoid analogs against CB1 and CB2 receptors. Comput Biol Chem. 2021;95. https://doi.org/10.1016/j.compbiolchem.2021.107590
32. Jung SW, Cho AE, Yu W. Exploring the ligand efficacy of cannabinoid receptor 1 (CB1) using molecular dynamics simulations. Sci Rep. 2018;8(1). https://doi.org/10.1038/s41598-018-31749-z
33. Ji B, Liu S, He X, Man VH, Xie XQ, Wang J. Prediction of the binding affinities and selectivity for CB1 and CB2 ligands using homology modeling, molecular docking, molecular dynamics simulations, and MM-PBSA binding free energy calculations. ACS Chem Neurosci. 2020;11(8):1139–58. https://doi.org/10.1021/acschemneuro.9b00696
34. Loo JSE, Yong AYY, Yong YN. The effect of multiple simulation parameters on MM/PBSA performance for binding affinity prediction of CB1 cannabinoid receptor agonists and antagonists. Chem Biol Drug Des. 2020;0–1. https://doi.org/10.1111/cbdd.13733
35. Loo JSE, Emtage AL, Murali L, Lee SS, Kueh ALW, Alexander SPH. Ligand discrimination during virtual screening of the CB1 cannabinoid receptor crystal structures following cross-docking and microsecond molecular dynamics simulations. RSC Adv. 2019;9(28):15949–56. https://doi.org/10.1039/C9RA01095E
36. Yau MQ, Emtage AL, Chan NJY, Doughty SW, Loo JSE. Evaluating the performance of MM/PBSA for binding affinity prediction using class A GPCR crystal structures. J Comput Aided Mol Des. 2019;33(5):487–96. https://doi.org/10.1007/s10822-019-00201-3
37. Wang E, Sun H, Wang J, Wang Z, Liu H, Zhang JZH, et al. End-point binding free energy calculation with MM/PBSA and MM/GBSA: Strategies and applications in drug design. Chem Rev [Internet]. 2019;119(16):9478–9508. http://pubs.acs.org/doi/10.1021/acs.chemrev.9b00055
38. Genheden S, Ryde U. The MM/PBSA and MM/GBSA methods to estimate ligand-binding affinities. Expert Opin Drug Discov. 2015;10(5):449–61. http://dx.doi.org/10.1517/17460441.2015.1032936
39. Mongan J, Simmerling C, McCammon JA, Case DA, Onufriev A. Generalized Born model with a simple, robust molecular volume correction. J Chem Theory Comput. 2007;3(1):156–69.

https://doi.org/10.1021/ct600085e

40. Yau MQ, Loo JSE. Consensus scoring evaluated using the GPCR-Bench dataset: Reconsidering the role of MM/GBSA. J Comput Aided Mol Des. 2022;36:427-41. https://doi.org/10.1007/s10822-022-00456-3
41. Yau MQ, Emtage AL, Loo JSE. Benchmarking the performance of MM/PBSA in virtual screening enrichment using the GPCR - Bench dataset. J Comput Aided Mol Des. 2020;34:1133-45. https://doi.org/10.1007/s10822-020-00339-5
42. Rastelli G, Pinzi L. Refinement and Rescoring of Virtual Screening Results. Front Chem. 2019;7:1–6. https://doi.org/10.3389/fchem.2019.00498
43. Wang Z, Sun H, Shen C, Hu X, Gao J, Li D, et al. Combined strategies in structure-based virtual screening. Physical Chemistry Chemical Physics. 2020;22:3149-59. https://doi.org/10.1039/C9CP06303J
44. Poli G, Granchi C, Rizzolio F, Tuccinardi T. Application of MM-PBSA methods in virtual screening. Molecules. 2020;25(8):1971. https://doi.org/10.3390/molecules25081971
45. Hou T, Wang J, Li Y, Wang W. Assessing the performance of the MM/PBSA and MM/GBSA methods: I. The accuracy of binding free energy calculations based on molecular dynamics simulations. J Chem Inf Model. 2011;51(1):69–82. https://doi.org/10.1021/ci100275a
46. Gaulton A, Hersey A, Nowotka ML, Patricia Bento A, Chambers J, Mendez D, et al. The ChEMBL database in 2017. Nucleic Acids Res. 2017;45(D1):D945–54. https://doi.org/10.1093/nar/gkw1074
47. LigPrep. New York: Schrödinger, LLC; 2018.
48. Rose PW, Prlić A, Bi C, Bluhm WF, Christie CH, Dutta S, et al. The RCSB Protein Data Bank: Views of structural biology for basic and applied research and education. Nucleic Acids Res. 2015;43(D1):D345–56. https://doi.org/10.1093/nar/gku1214
49. Maestro. New York: Schrödinger, LLC; 2018.
50. Shelley JC, Cholleti A, Frye LL, Greenwood JR, Timlin MR, Uchimaya M. Epik: A software program for pKa prediction and protonation state generation for drug-like molecules. J Comput Aided Mol Des. 2007;21(12):681–91. https://doi.org/10.1007/s10822-007-9133-z
51. Sherman W, Beard HS, Farid R. Use of an Induced Fit Receptor Structure in Virtual Screening. Chem Biol Drug Des. 2006;67(1):83–4. https://doi.org/10.1111/j.1747-0285.2005.00327.x
52. Sherman W, Day T, Jacobson MP, Friesner RA, Farid R. Novel Procedure for Modeling Ligand/Receptor Induced Fit Effects. J Med Chem. 2006;49(2):534–53. https://doi.org/10.1021/jm050540c
53. Abraham MJ, Hess B, van der Spoel D, Lindahl E. GROMACS User Manual version 2018. 2018.
54. Lindorff-Larsen K, Piana S, Palmo K, Maragakis P, Klepeis JL, Dror RO, et al. Improved side-chain torsion potentials for the Amber ff99SB protein force field. Proteins: Structure, Function and Bioinformatics. 2010;78(8):1950–8. https://doi.org/10.1002/prot.22711

55. Wang J, Wolf RM, Caldwell JW, Kollman PA, Case DA. Development and testing of a general Amber force field. J Comput Chem. 2004;25(9):1157–74. https://doi.org/10.1002/jcc.20035
56. Jämbeck JPM, Lyubartsev AP. Derivation and systematic validation of a refined all-atom force field for phosphatidylcholine lipids. Journal of Physical Chemistry B. 2012;116(10):3164–79. https://doi.org/10.1021/jp212503e
57. Jakalian A, Jack DB, Bayly CI. Fast, efficient generation of high-quality atomic charges. AM1-BCC model: II. Parameterization and validation. J Comput Chem. 2002;23(16):1623–41. https://doi.org/10.1002/jcc.10128
58. Sousa da Silva AW, Vranken WF. ACPYPE - AnteChamber PYthon Parser interfacE. BMC Res Notes. 2012;5(1):367. https://doi.org/10.1186/1756-0500-5-367
59. Darden T, York D, Pedersen L. Particle mesh Ewald: An N log(N) method for Ewald sums in large systems. J Chem Phys. 1993;98(12):10089–92. https://doi.org/10.1063/1.464397
60. Hess B, Bekker H, Berendsen HJC, Fraaije JGEM. LINCS: A linear constraint solver for molecular simulations. J Comput Chem. 1997;18(12):1463–72. https://doi.org/10.1002/(SICI)1096-987X(199709)18:12%3C1463::AID-JCC4%3E3.0.CO;2-H
61. Hess B. P-LINCS: A parallel linear constraint solver for molecular simulation. J Chem Theory Comput. 2008;4(1):116–22. https://doi.org/10.1021/ct700200b
62. Nugent T, Jones DT. Membrane protein orientation and refinement using a knowledge-based statistical potential. BMC Bioinformatics. 2013;14:276. https://doi.org/10.1186/1471-2105-14-276
63. Wu EL, Cheng X, Jo S, Rui H, Song KC, Dávila-Contreras EM, et al. CHARMM-GUI membrane builder toward realistic biological membrane simulations. Journal of Computational Chemistry. John Wiley and Sons Inc.; 2014;35(27):1997–2004. https://doi.org/10.1002/jcc.23702
64. Jorgensen WL, Chandrasekhar J, Madura JD, Impey RW, Klein ML. Comparison of simple potential functions for simulating liquid water. J Chem Phys. 1983;79(2):926–35. https://doi.org/10.1063/1.445869
65. Berendsen HJC, Postma JPM, van Gunsteren WF, DiNola A, Haak JR. Molecular dynamics with coupling to an external bath. J Chem Phys. 1984;81(8):3684–90. https://doi.org/10.1063/1.448118
66. Nosé S, Klein ML. Constant pressure molecular dynamics for molecular systems. Molecular Physics: An International Journal at the Interface Between Chemistry and Physics. 1983;50(5):1055–76. https://doi.org/10.1080/00268978300102851
67. Bussi G, Donadio D, Parrinello M. Canonical sampling through velocity-rescaling. Journal of Chemical Physics. 2007;126(1):1–8. https://doi.org/10.1063/1.2408420
68. Valdés-Tresanco MS, Valdés-Tresanco ME, Valiente PA, Moreno E. gmx_MMPBSA: A New Tool to Perform End-State Free Energy Calculations with GROMACS. J Chem Theory Comput. 2021;17(10):6281–6291. https://doi.org/10.1021/acs.jctc.1c00645
69. Onufriev A, Bashford D, Case DA. Exploring Protein Native States and Large-Scale Conformational Changes with a Modified Generalized Born Model. Proteins: Structure, Function and Genetics. 2004;55(2):383–94. https://doi.org/10.1002/prot.20033

70. Hawkins GD, Cramer CJ, Truhlar DG. Pairwise solute descreening of solute charges from a dielectric medium. Chem Phys Lett. 1995;246(1–2):122–9. https://doi.org/10.1016/0009-2614(95)01082-K
71. Nguyen H, Roe DR, Simmerling C. Improved generalized born solvent model parameters for protein simulations. J Chem Theory Comput. 2013;9(4):2020–34. https://doi.org/10.1021/ct3010485
72. Kashefolgheta S, Wang S, Acree WE, Hünenberger PH. Evaluation of nine condensed-phase force fields of the GROMOS, CHARMM, OPLS, AMBER, and OpenFF families against experimental cross-solvation free energies. Physical Chemistry Chemical Physics. 2021;23(23):13055–74. https://doi.org/10.1039/D1CP00215E
73. Shivakumar D, Williams J, Wu Y, Damm W, Shelley J, Sherman W. Prediction of absolute solvation free energies using molecular dynamics free energy perturbation and the OPLS force field. J Chem Theory Comput. 2010;6(5):1509–19. https://doi.org/10.1021/ct900587b
74. Sun H, Li Y, Shen M, Tian S, Xu L, Pan P, et al. Assessing the performance of MM/PBSA and MM/GBSA methods. 5. Improved docking performance by using high solute dielectric constant MM/GBSA and MM/PBSA rescoring. Physical Chemistry Chemical Physics. 2014;16:22035–45. https://doi.org/10.1039/C4CP03179B
75. Hou T, Wang J, Li Y, Wang W. Assessing the performance of the MM/PBSA and MM/GBSA methods: II. The accuracy of ranking poses generated from docking. J Comput Chem. 2011;32(5):866–77. https://doi.org/10.1002%2Fjcc.21666
76. Sun H, Li Y, Tian S, Xu L, Hou T. Assessing the performance of MM/PBSA and MM/GBSA methods. 4. Accuracies of MM/PBSA and MM/GBSA methodologies evaluated by various simulation protocols using PDBbind data set. Physical Chemistry Chemical Physics. 2014;16(31):16719. https://doi.org/10.1039/C4CP01388C
77. Yang T, Wu JC, Yan C, Wang Y, Luo R, Gonzales MB, et al. Virtual screening using molecular simulations. Proteins. 2011;79(6):1940–51. https://doi.org/10.1002/prot.23018
78. Chéron N, Shakhnovich EI. Effect of sampling on BACE-1 ligands binding free energy predictions via MM-PBSA calculations. J Comput Chem. 2017;38(22):1941–51. https://doi.org/10.1002/jcc.24839
79. Zhang X, Perez-Sanchez H, Lightstone FC. A comprehensive docking and MM/GBSA rescoring study of ligand recognition upon binding antithrombin. Curr Top Med Chem. 2017;17:1631–9. https://doi.org/10.2174/1568026616666161117112604
80. Rastelli G, Rio A Del, Degliesposti G, Sgobba M. Fast and accurate predictions of binding free energies using MM-PBSA and MM-GBSA. J Comput Chem. 2010;31:797–810. https://doi.org/10.1002/jcc.21372
81. Guimarães CRW. A Direct Comparison of the MM-GB/SA Scoring Procedure and Free-Energy Perturbation Calculations Using Carbonic Anhydrase as a Test Case: Strengths and Pitfalls of Each Approach. J Chem Theory Comput. 2011;7:2296–306. https://doi.org/10.1021/ct200244p
82. Mikulskis P, Genheden S, Rydberg P, Sandberg L, Olsen L, Ryde U. Binding affinities in the SAMPL3 trypsin and host-guest blind tests estimated with the MM/PBSA and LIE methods. J Comput Aided Mol Des. 2012;26(5):527–41. https://doi.org/10.1007/s10822-011-9524-z

83. Li Y, Cong Y, Feng G, Zhong S, Zhang JZH, Sun H, et al. The impact of interior dielectric constant and entropic change on HIV-1 complex binding free energy prediction. Structural Dynamics. 2018;5(6):1–22. http://dx.doi.org/10.1063/1.5058172
84. Genheden S, Kuhn O, Mikulskis P, Hoffmann D, Ryde U. The normal-mode entropy in the MM/GBSA method: Effect of system truncation, buffer region, and dielectric constant. J Chem Inf Model. 2012;52(8):2079–88. https://doi.org/10.1021/ci3001919
85. Sheng YJ, Yin YW, Ma YQ, Ding HM. Improving the Performance of MM/PBSA in Protein-Protein Interactions via the Screening Electrostatic Energy. J Chem Inf Model. 2021;61(5):2454–62. https://doi.org/10.1021/acs.jcim.1c00410
86. Liu X, Peng L, Zhang JZH. Accurate and Efficient Calculation of Protein-Protein Binding Free Energy-Interaction Entropy with Residue Type-Specific Dielectric Constants. J Chem Inf Model. 2019;59(1):272–81. https://doi.org/10.1021/acs.jcim.8b00248
87. Duan L, Liu X, Zhang JZH. Interaction entropy: A new paradigm for highly efficient and reliable computation of protein-ligand binding free energy. J Am Chem Soc. 2016;138(17):5722–8. https://doi.org/10.1021/jacs.6b02682
88. Suárez D, Díaz N. Affinity Calculations of Cyclodextrin Host-Guest Complexes: Assessment of Strengths and Weaknesses of End-Point Free Energy Methods. J Chem Inf Model. 2019 Jan 28;59(1):421–40. https://doi.org/10.1021/acs.jcim.8b00805
89. Zeller F, Zacharias M. Evaluation of generalized born model accuracy for absolute binding free energy calculations. Journal of Physical Chemistry B. 2014;118(27):7467–74. https://doi.org/10.1021/jp5015934
90. Izadi S, Harris RC, Fenley MO, Onufriev A V. Accuracy Comparison of Generalized Born Models in the Calculation of Electrostatic Binding Free Energies. J Chem Theory Comput. 2018;14(3):1656–70. https://doi.org/10.1021/acs.jctc.7b00886
91. Su PC, Tsai CC, Mehboob S, Hevener KE, Johnson ME. Comparison of radii sets, entropy, QM methods, and sampling on MM-PBSA, MM-GBSA, and QM/MM-GBSA ligand binding energies of F. tularensis enoyl-ACP reductase (FabI). J Comput Chem. 2015;36(25):1859–73. https://doi.org/10.1002/jcc.24011
92. Shell MS, Ritterson R, Dill KA. A test on peptide stability of AMBER force fields with implicit solvation. Journal of Physical Chemistry B. 2008;112(22):6878–86. https://doi.org/10.1021/jp800282x

Figures

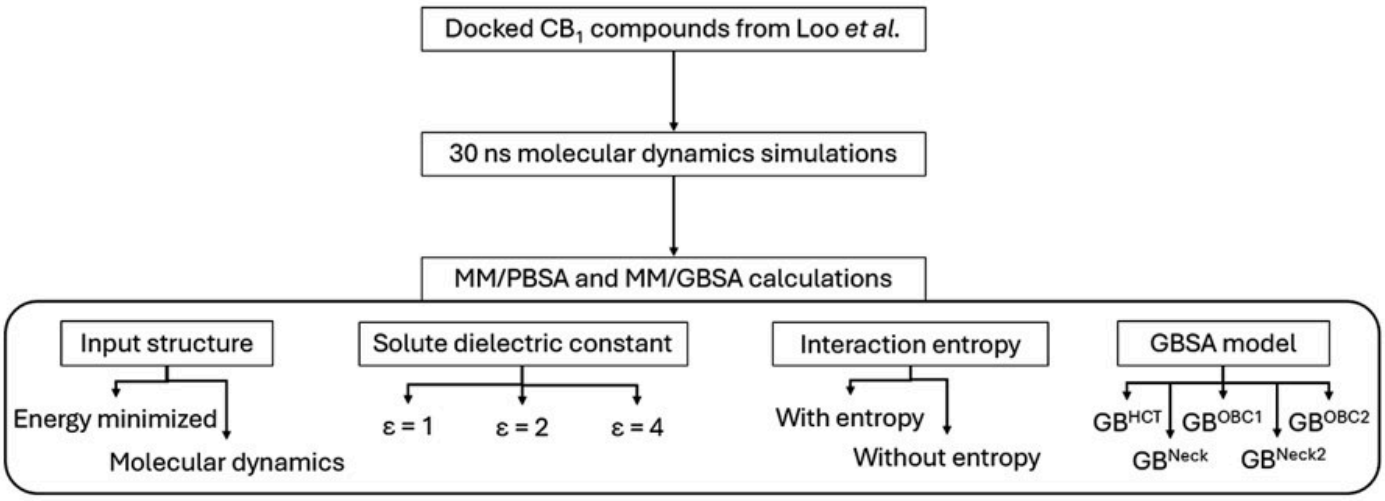


Figure 1

Flowchart of MM/PBSA and MM/GBSA calculations using various parameters.

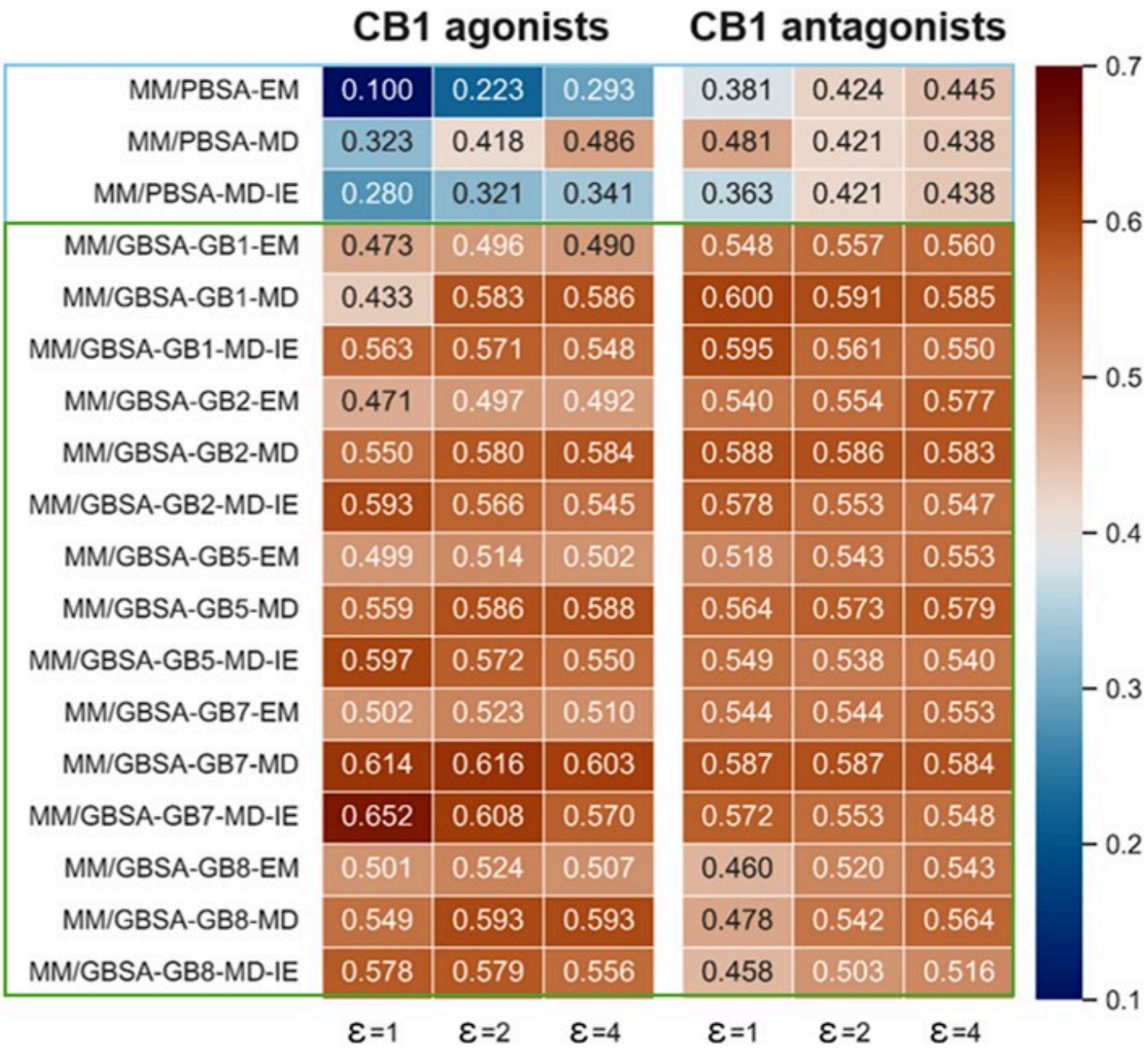


Figure 2

Heatmap of correlations obtained by MM/PBSA and MM/GBSA for CB_1 agonists and CB_1 antagonists.

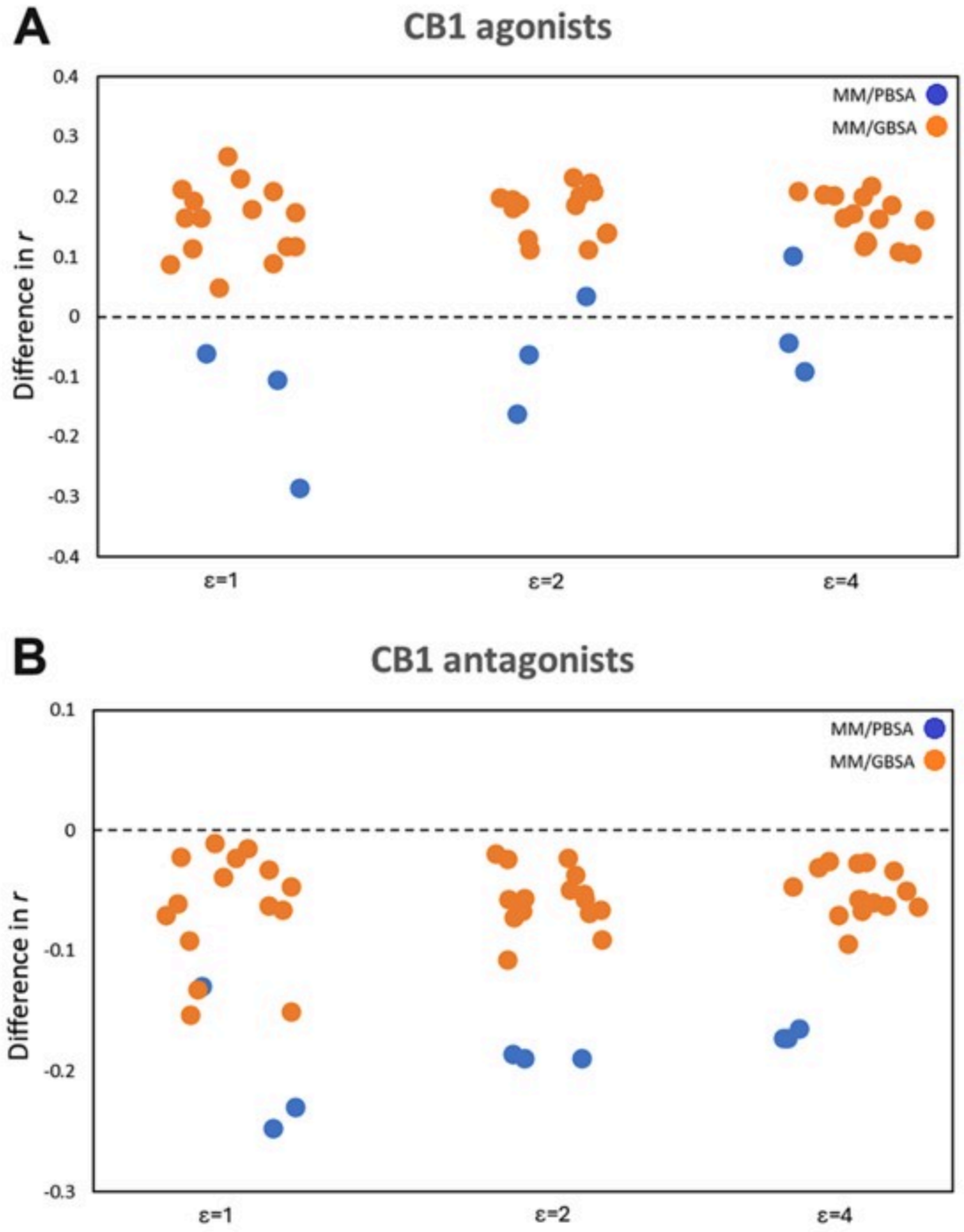


Figure 3

Differences in correlation coefficients, *r*, for MM/PBSA and MM/GBSA in comparison to Glide for a) CB1 agonists, and b) CB1 antagonists.